the FEBS Journal

Novel biosensors based on optimized glycine oxidase

Elena Rosini[1,2], Luciano Piubelli[1,2], Gianluca Molla[1,2], Luca Frattini[1], Mattia Valentino[2,3], Antonio Varriale[4], Sabato D'Auria[4] and Loredano Pollegioni[1,2]

1 Dipartimento di Biotecnologie e Scienze della Vita, Università degli studi dell'Insubria, Varese, Italy
2 The Protein Factory, Centro Interuniversitario di Biotecnologie Proteiche, Politecnico di Milano, ICRM CNR Milano, Università degli studi dell'Insubria, Milano, Italy
3 CNR – Istituto di Chimica del Riconoscimento Molecolare, Sezione Adolfo Quilico, Milano, Italy
4 CNR – Istituto di Biochimica delle Proteine, Napoli, Italy

Keywords
biosensor; flavoprotein; glycine; protein engineering; sarcosine

Correspondence
E. Rosini, The Protein Factory, Centro Interuniversitario di Biotecnologie Proteiche, via Mancinelli 7, 20131 Milano, Italy
Fax: +39 0332421500
Tel: +39 0223993062
E-mail: elena.rosini@uninsubria.it

(Received 26 March 2014, revised 27 May 2014, accepted 9 June 2014)

doi:10.1111/febs.12873

Glycine is involved in several physiological functions, e.g. as a neurotransmitter in the central nervous system, and sarcosine has been identified as a differential metabolite greatly enhanced during prostate cancer progression and metastasis. Glycine oxidase from *Bacillus subtilis* (GO) was engineered with the final aim of producing specific analytical systems to detect these small achiral amino acids. Based on *in silico* analysis, site-saturation mutagenesis was independently performed at 11 positions: a total of 16 single-point GO variants were analyzed. Significantly improved kinetic parameters were observed on glycine for the A54R, H244K-N-Q-R, Y246W and M261R variants. The introduction of multiple mutations then identified the H244K/M261R variant showing a 5.4-fold increase in maximal activity on glycine. With sarcosine as substrate, a number of single-point variants showed increased maximal activity and/or affinity: the kinetic efficiency was increased 6-fold for the M49L variant. Two GO variants with a high substrate specificity ratio for glycine (versus sarcosine, i.e. H244K GO) or for sarcosine (versus glycine, i.e. M49L GO) combined with high substrate affinity were used to set up a simple fluorescence-based biosensor. This optical sensing assay represents a novel, inexpensive and fast tool to assay glycine or sarcosine concentrations in biological samples (detection limit ≤ 0.5 μM).

Introduction

Glycine is the smallest and the only nonchiral natural α-amino acid used for protein biosynthesis. In addition to such a structural role, it possesses further physiological functions: it is an important biosynthetic precursor (i.e. it is used for *de novo* synthesis of porphyrins and purines) and it acts as a neurotransmitter in the central nervous system. Glycine is a coagonist, together with D-serine, of glutamate at glutamatergic *N*-methyl-D-aspartate receptors (NMDARs) in the forebrain [1], thus serving both inhibitory and excitatory functions [2]. Due to this role, glycine is probably involved in the pathophysiology of schizophrenia and other neurological diseases. For example, a correlation exists between low levels of glycine and catatonia (a psychiatric disease), and the perturbation of the glycine deportation system is associated with ifosfamide encephalopathy and congenital nonketotic hyperglycinemia [2].

Sarcosine, 2-(methylamino)acetic acid or *N*-methylglycine, is a natural, small, endogenous amino acid present in low concentrations in the blood and in urine. It has been proposed to play a role in the progression of prostate cancer, and assessing sarcosine concentrations in body fluids was suggested as a novel biomarker for prostate cancer [3].

Abbreviations
DAAO, D-amino acid oxidase; GO, glycine oxidase; NMDAR, *N*-methyl-D-aspartate receptor; *o*DNS, *o*-dianisidine.

With the final aim of developing a biosensor to assay glycine and sarcosine in biological fluids, we engineered glycine oxidase from *Bacillus subtilis* (GO) (EC 1.4.3.19) to improve its kinetic efficiency on these two compounds. GO is a homotetrameric flavoenzyme that contains one molecule of noncovalently bound FAD per 47 kDa protein monomer [4,5]. Purified recombinant GO catalyzes the oxidative deamination of various primary and secondary amines (e.g. glycine and sarcosine) and D-amino acids (e.g. D-alanine and D-proline) to yield the corresponding α-imino acids and, after hydrolysis, α-keto acids, ammonia (or primary amines) and hydrogen peroxide [4,5]. Compared with similar amino acid flavoprotein oxidases [6,7], the activity ($k_{cat,app}$ is 0.6 s^{-1}) and kinetic efficiency ($k_{cat,app}/K_{m,app}$ is 860 $M^{-1}{\cdot}s^{-1}$ on the physiological substrate glycine) of GO are low. The crystal structure of GO was solved as a complex with the inhibitor glycolate up to 1.8 Å resolution [8,9]: GO is a member of the glutathione reductase family (subfamily GR2) of FAD-containing oxidases, a family of flavoproteins on which a number of important biotechnological applications have been based [10]. Most recently, a GO variant active on the herbicide glyphosate was generated in a semi-rational protein-engineering study [11], thus demonstrating that the substrate preference of this flavoenzyme can be evolved.

Here, we report on a protein-engineering approach (based on site-saturation and site-directed mutagenesis) to generate GO variants with improved kinetic properties on glycine and sarcosine and applied them to develop a simple and inexpensive fluorescence-based biosensor.

Results

Docking analysis on wild-type GO

In order to obtain details on the mode of glycine and sarcosine binding at the active site of wild-type GO, a molecular docking analysis was performed. Analysis of the complex between glycine and the flavoprotein suggests that the small substrate binds to the enzyme active site in the canonical way, as already observed for other amino acid oxidases [6,7], forming a two-point interaction with the side chain of the active site Arg302. Thus the αC is at 3.3 Å from the flavin N5, an optimal distance for hydride transfer. On the basis of the *in silico* analysis, several residues in the first and second shell of the GO active site were identified as potential targets for mutagenesis (Fig. 1).

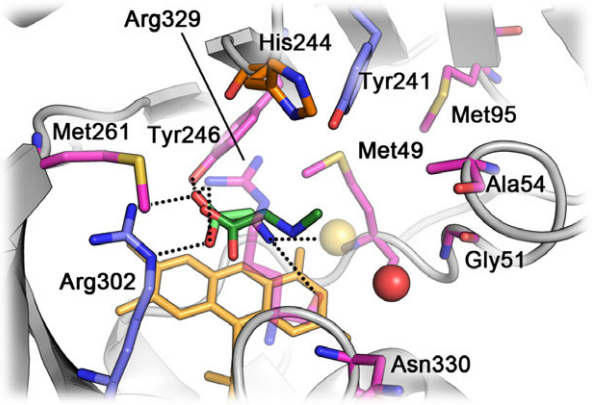

Fig. 1. Docking of glycine (pale green) and sarcosine (dark green) at the active site of wild-type GO. The water molecule that was removed in the dockings with sarcosine is shown in pale yellow. Putative H-bonds between glycine and active site residues are represented by dotted lines. Residues involved in mutagenesis are represented in sticks and colored by their conservation scores: purple, conserved residues; blue, conservation scores > 70%; orange, conservation scores > 35%. See text for details.

Selection of GO variants obtained by site-saturation mutagenesis on glycine as substrate

Site-saturation mutagenesis experiments were independently performed at positions Met49, Gly51, Ala54, Met95, Tyr241, His244, Tyr246, Met261, Arg302, Arg329 and Asn330 (Fig. 1, Table 1) using the QuikChange kit and the wild-type GO cDNA as template. The GO variants were screened for activity on 1.8 mM glycine by the peroxidase-*o*-dianisidine (*o*DNS) colorimetric assay reported in Experimental procedures (using a microtiter plate and an automated liquid-handler system). The clones most active on glycine, as detected via the screening procedure, were isolated and the mutations were identified by automatic DNA sequencing. None of the clones from site-saturation mutagenesis at positions 95, 241, 302 and 329 showed an activity on glycine higher than the wild-type GO (Table 1). Interestingly, the substitution of Arg302 was associated with the complete abolition of enzymatic activity (the only active variants were wild-type clones; data not shown), thus confirming a primary role for such a residue in substrate binding [8].

Characterization of GO variants

Thirteen selected GO variants identified by the screening procedure on glycine as substrate were expressed in BL21(DE3)pLysS *Escherichia coli* cells and purified by nickel-affinity chromatography on a HiTrap chelating column (≥ 90% purity). For all protein variants,

Table 1. Amino acid substitutions in GO variants obtained by site-saturation mutagenesis and identified by the peroxidase-*o*DNS colorimetric screening procedure on glycine or sarcosine (*) as substrate.

Starting GO variant	Amino acid position	Introduced substitution
Wild-type	M49	I*, L, T*
	G51	H, I, Q
	A54	E, R
	M95	–
	Y241	–
	H244	A*, Q, R, K
	Y246	W
	M261	I, R
	R302	–
	R329	–
	N330	P
H244K	M49	–
	A54	–
	Y246	–
A54R/H244K	M49	–

the expression yield was lower than for wild-type GO (7–15 $mg \cdot L^{-1}$ of pure protein versus 40 $mg \cdot L^{-1}$, respectively). The visible absorption spectrum of the purified GO variants in the oxidized state was similar to that of the wild-type enzyme (not shown); the estimated flavin absorption coefficient of the main peak at 455 nm was in the 11.3–15.0 $mM^{-1} \cdot cm^{-1}$ range. The only exception here was the substitution of Asn330 with a proline; this recombinant GO variant was isolated in the apoprotein form, showing no activity on glycine (or sarcosine, see below) even in the presence of a 10-fold molar excess of FAD in the assay mixture.

The apparent kinetic parameters at 21% oxygen saturation ($k_{cat,app}$ and $K_{m,app}$ values) were determined for wild-type and variants of GO on glycine or sarcosine as substrates using the oxygen consumption assay (Table 2). In comparison with the kinetic parameters of wild-type GO, an increase in activity was observed on glycine for the A54R, H244K-N-Q-R, Y246W and M261R variants (2.5-fold higher $k_{cat,app}$ for the H244R GO) and a decreased $K_{m,app}$ for the M49I and H244K-R variants. Kinetic efficiency ($k_{cat,app}/K_{m,app}$) increased from 860 $M^{-1} \cdot s^{-1}$ for the wild-type to 9650 $M^{-1} \cdot s^{-1}$ for the H244K GO variant (see Table 2 and Fig. 2A).

Due to the importance of assaying sarcosine (see the Introduction), the activity of GO variants was also assessed on this substrate. The highest increase in the specificity constant was observed for M49L GO (because of an ~ 6-fold increase in substrate affinity) and a 2-fold increase in $k_{cat,app}$ was apparent for G51H, A54R, H244K-N-R and M261I (Table 2 and Fig. 2). With regard to the H244 GO variants, the increased activity observed with glycine was also apparent on sarcosine although a decrease in $K_{m,app}$ was not observed with the largest substrate. Increased activity on sarcosine was also evident for G51H-I variants. The kinetic characterization of GO variants suggests that positions 49 and 244 play a main role in determining the affinity and activity for sarcosine. Therefore, the GO libraries obtained from site-saturation mutagenesis at these positions were re-screened on 1.8 mM sarcosine. From the screening procedure, the H244A and M49T-I-L GO variants were selected (the latter two were also identified by the previous screening on glycine). The H244A variant showed a 1.7-fold increase in maximal enzymatic activity and the M49T GO exhibited a 4.4-fold increase in sarcosine affinity. It is remarkable that the M49I, M49L and H244A GO variants were also identified during the previous screening in search for a GO more active on glyphosate, a broad-spectrum herbicide [11].

Introduction of multiple substitutions

As shown in Table 2 and Fig. 2, the highest kinetic efficiency for glycine is observed for the H224K and H244R GO variants (these variants showing a very low $K_{m,app}$ value) and the highest k_{cat} for the A54R, H244K-N-Q-R, Y246W and M261R GO variants. Compared with wild-type enzyme, the $k_{cat,app}$ parameter for sarcosine as substrate is increased for most of the identified variants, the main exceptions being the ones at position M49 (which show a lower $K_{m,app}$ anyway) and the A54E GO (Table 2). Altogether, the kinetic results suggest that positions 49, 54 and 246 play a main role in the GO substrate preference. Therefore, site-saturation mutagenesis at these three positions was carried out using the cDNA encoding for the H244K GO variant as template and, subsequently, position 49 was saturated starting from the cDNA encoding for the A54R/H244K GO variant (see Table 1). Unfortunately, no improved GO variants on glycine as substrate were identified upon screening of the corresponding libraries (Table 1).

Subsequently, the amino acid substitutions found in the GO variants with improved activity as obtained by site-saturation mutagenesis were combined; the double A54R/H244K and H244K/M261R, as well as the triple M49L/A54R/H244K and A54R/H244K/M261R GO variants, were prepared by site-directed mutagenesis. It is noteworthy that the H244K/M261R GO variant shows similar (and improved if compared with

Table 2. Comparison of the apparent kinetic parameters (determined at 21% oxygen saturation) on glycine or sarcosine as substrates for wild-type and variants of GO obtained by site-directed and site-saturation mutagenesis experiments. The values showing most significant changes are in bold. b.d., below detection.

	Glycine			Sarcosine		
	$k_{cat,app}$ (s^{-1})	$K_{m,app}$ (mM)	$k_{cat,app}/K_{m,app}$	$k_{cat,app}$ (s^{-1})	$K_{m,app}$ (mM)	$k_{cat,app}/K_{m,app}$
Wild-type	0.60 ± 0.03	0.70 ± 0.10	0.86	0.60 ± 0.02	0.70 ± 0.10	0.86
Site-saturation mutagenesis						
M49I	0.36 ± 0.01	**0.31 ± 0.09**	1.17	0.38 ± 0.01	**0.22 ± 0.04**	1.75
M49L	0.43 ± 0.04	1.35 ± 0.35	0.32	0.63 ± 0.03	**0.12 ± 0.05**	**5.21**
M49T	0.04 ± 0.01	1.47 ± 0.17	0.03	0.11 ± 0.01	**0.16 ± 0.01**	0.69
G51H	0.77 ± 0.04	35.7 ± 4.48	0.02	1.25 ± 0.06	2.38 ± 0.41	0.53
G51I		b.d.		1.02 ± 0.04	2.87 ± 0.34	0.35
G51Q	0.74 ± 0.04	14.6 ± 1.90	0.05	0.82 ± 0.05	5.00 ± 0.90	0.16
A54E	0.35 ± 0.02	10.0 ± 1.56	0.04	0.24 ± 0.02	5.90 ± 1.30	0.04
A54R[a]	1.20 ± 0.10	28.0 ± 3.00	0.04	1.30 ± 0.07	20.5 ± 2.21	0.06
H244A	0.63 ± 0.06[a]	1.50 ± 0.30[a]	0.42[a]	1.00 ± 0.02	1.81 ± 0.14	0.55
H244K	1.35 ± 0.05	**0.14 ± 0.02**	**9.65**	1.14 ± 0.05	0.78 ± 0.17	1.46
H244N[b]	1.30 ± 0.05	1.90 ± 0.21	0.68	1.33 ± 0.06	2.10 ± 0.40	0.63
H244Q	1.21 ± 0.06	0.90 ± 0.04	1.34	1.07 ± 0.06	2.20 ± 0.40	0.49
H244R	1.49 ± 0.06	**0.24 ± 0.20**	**6.22**	1.21 ± 0.04	0.84 ± 0.15	1.44
Y246W	1.21 ± 0.14	17.2 ± 3.40	0.07	0.87 ± 0.05	5.90 ± 0.90	0.15
M261I	0.64 ± 0.04	1.50 ± 0.30	0.43	1.14 ± 0.07	0.60 ± 0.20	1.90
M261R	1.00 ± 0.04	3.50 ± 0.30	0.30	0.90 ± 0.02	1.63 ± 0.15	0.53
Site-directed mutagenesis						
A54R/H244K	**3.20 ± 0.21**	40.1 ± 6.40	0.11	**4.40 ± 0.70**	20.2 ± 7.40	0.22
H244K/M261R	1.20 ± 0.02	**0.30 ± 0.03**	**4.00**	1.10 ± 0.11	**0.28 ± 0.10**	**3.93**
M49L/A54R/H244K	0.6 ± 0.01	18.8 ± 3.20	0.03	0.73 ± 0.06	1.48 ± 0.34	0.50
A54R/H244K/M261R	1.61 ± 0.02	45.9 ± 2.50	0.04	**2.80 ± 0.60**	59.0 ± 24.0	0.05

[a] [11].
[b] [24].

wild-type GO) kinetic properties on both glycine and sarcosine (see Table 2). A huge increase in $k_{cat,app}$ on both the substrates tested is apparent for the A54R/H244K variant but coupled to a lower affinity, which negatively affects the kinetic efficiency; this result points to a synergistic effect of the coupled, selected substitutions on the maximal activity of GO. When the A54R, H244K and M261R substitutions are simultaneously introduced, a lower $k_{cat,app}$ compared with the A54R/H244K variant and a higher $K_{m,app}$ compared with the H244K/M261R GO are apparent. The substrate affinity for both glycine and sarcosine (up to 13.6-fold on sarcosine) could be increased to a significant extent by further introducing the M49L substitution in the A54R/H244K GO variant but at the detriment of k_{cat} (reaching values comparable with those of the single-point M49L GO).

To compare the temperature sensitivity of wild-type GO and its more interesting variants, temperature ramp experiments were performed in which changes in the protein fluorescence were detected as a probe of protein (un)folding [12,13]. The introduction of a positively charged side chain at position 54 (i.e. A54R) or at position 244 (i.e. H244K-R substitutions) produced a 12 °C and 7 °C decreased midpoint transition temperature (T_m) compared with the wild-type GO (Table 3).

Phylogenetic analyses

The evolutionary conservation of amino acid positions in the GO enzyme was investigated by comparing its sequence with those of evolutionarily related enzymes, removing redundant sequences and setting the minimal percentage for homologs to 30% [14]. The phylogenetic tree was constructed and the most probable ancestral sequences of various nodes that connect the paralogous families were predicted as described in Experimental procedures (Fig. 3A). In order to understand the biological importance of each saturated sequence position, the alignment between the predicted most probable ancestral sequence of node 5 and the GO wild-type sequence (43% identity) was constructed and the conservation score for each position was

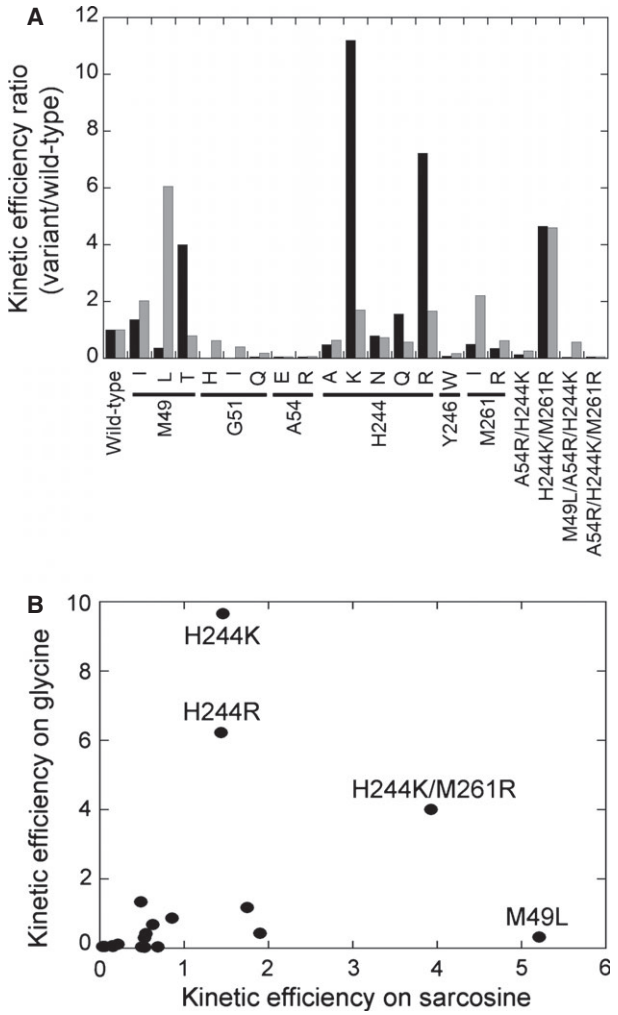

Fig. 2. (A) Comparison of the specificity ratio (the ratio between $k_{cat,app}/K_{m,app}$ variant and $k_{cat,app}/K_{m,app}$ wild-type) on glycine (black) and sarcosine (gray) for the selected GO variants. (B) Dot plot reporting the kinetic efficiency on glycine versus sarcosine of all the GO variants identified in this work (see Table 2).

Table 3. Comparison of T_m values for unfolding of wild-type and evolved variants of GO as determined by following protein fluorescence changes during temperature ramp experiments.

	T_m (°C)
Wild-type[a]	56.9 ± 0.18
M49L	59.7 ± 0.03
A54R[b]	44.8 ± 0.30
H244K	50.0 ± 1.00
H244R	49.7 ± 0.40
M261I	53.9 ± 0.05
A54R/H244K	44.1 ± 0.09
H244K/M261R	53.2 ± 0.06

[a] [13].
[b] [11].

calculated. It is noteworthy that, H244 is the most variable position (Figs 1 and 3B): GO variants identified by the screening procedure at this position show a notable substrate specificity change (see Table 2). In the predicted ancestral amino acid sequence, an asparagine residue is present at position 244 (Fig. 3B). Interestingly, the introduction of a basic residue at this site results in GO variants that are more efficient on glycine than the wild-type enzyme (i.e. H244K and H244R variants, see Table 2).

Structure–function relationships in GO: comparison between docking analyses and kinetic properties

The estimated K_d values obtained from docking analysis (Table 4) for the complexes between wild-type GO and glycine or sarcosine are in good agreement with the experimentally determined $K_{m,app}$ figures (1.4 versus 1.35 mM and 0.9 versus 0.7 mM, respectively). It is important to point out that each glycine molecule can form a total of eight hydrogen bonds (five as acceptor and three as donor, both in the neutral or zwitterionic form) and that these are all fulfilled in the docked complex. In addition, due to the small and charged nature of the ligand, van der Waals interactions are thought to play only a marginal role in binding energy. For this reason, it is plausible that there is little chance to improve to a significant extent the thermodynamic affinity (at equilibrium) of GO for glycine by altering the active site, i.e. by mutagenesis. Accordingly, in docking simulations the estimated binding energy of wild-type GO for glycine (-3.9 kcal·mol^{-1}) could only be marginally improved (up to -4.1 kcal·mol^{-1}) by slightly altering active site side chain conformations or even by modeling an additional water molecule at an H-bond distance from the αNH_2 group of glycine (Table 4). The same analysis performed with sarcosine as the ligand obtained similar results; the estimated binding energy between wild-type GO and sarcosine was -4.1 kcal·mol^{-1}.

In an attempt to find a structural rationale for the increased affinity of H244K and M49L GO for glycine and sarcosine, respectively, docking analyses were performed using a structural model of the variant enzymes; see Experimental procedures. Residue H244 is ~ 7 Å from the ligand and separated from it by the side chains of residues R329 and Y241 (Fig. 1). Accordingly, it is not plausible that a mutation at this position would directly influence substrate binding (although the disposition of the active site waters was altered). In fact, docking of glycine or sarcosine to the H244K GO variant resulted in binding modes and

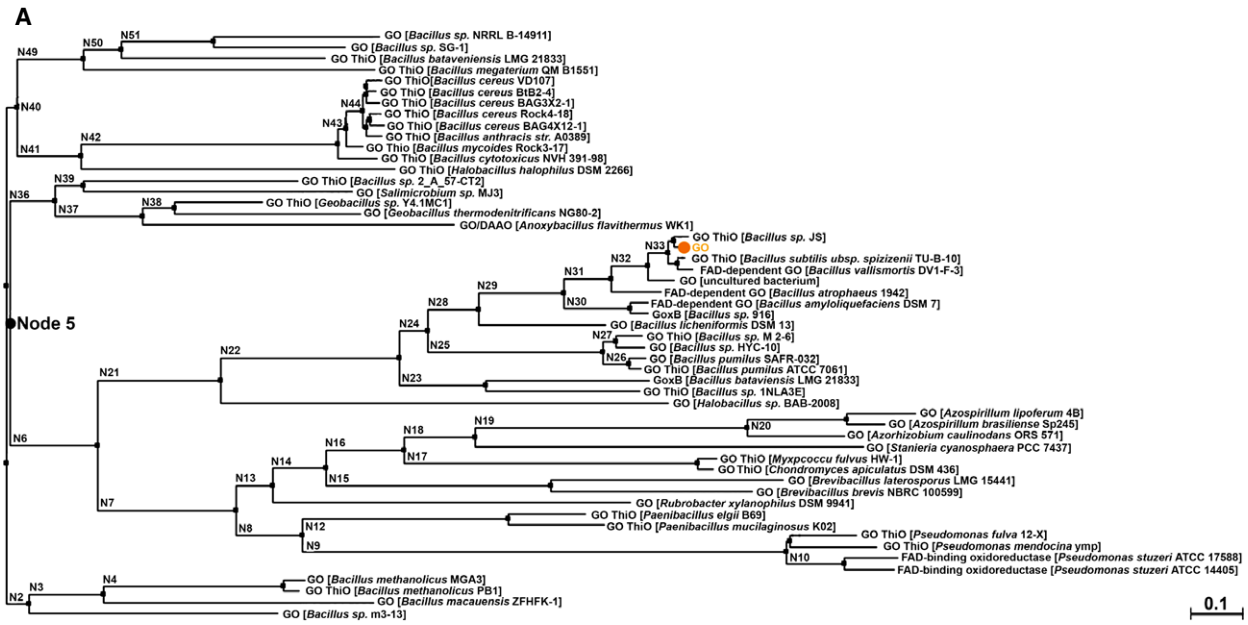

B

```
GO        MKR-HYEAVVIGGGIIGSAIAYYLAKEN-KNTALFESGTMGGRTTSAAAGMLGAHAECE- 57
Node 5    MNRKHYDVIIVGGGVIGCSIAYHLAKYRGHRVAILEKGRIGCEASSAAAGMLGAQAEIDG 60

GO        ERDAFFDFAMHSQRLYKGLGEELYALSGVDIRQHNGGMFKLAFSEEDVLQLR------QM 111
Node 5    EEGPLFELARKSRAMFPSLAEELKELSGIDIELVQKGMLKVALNEEEAQQLKRIIAFQQK 120

GO        DDLDSVSWYS-KEEVLEKEPYASG-DIFGASFIQDDVHVEPYFVCKAYVKA-AKMLGAEI 168
Node 5    ITGEQAEWLSNAEELREREPHLSNNALVGAMYIPNDGHVNAPELTRAFARALAAILGAEI 180

GO        FEHTPVLHVERD---GEALFIKTPSGDVWANHVVVASGVWSGMFFK-QLGLNNAFLPVKG 224
Node 5    REYTEVYDIIMEPGNERVVGVKTSQGEFYAETVVVAAGAWSGQLLQLQTGLSLPMYPVKG 240

GO        ECLSVWNDDIP--LTKTLYHDH-CYIVPRKSGRLVVGATMKPGDWSETPDLGGLESVMKK 281
Node 5    ECFSVKMDTEKPLLQSTIFSENGCYIVPKRGGRLIIGATMKPHTFDKKVTVGGISSLLEK 300

GO        AKTMLPAIQNMKVDRFWAGLRPGTKDGKPYIGRHPEDSRILFAAGHFRNGILLAPATGAL 341
Node 5    ATRLLPALKEAEWEKAWAGIRPQTGDGLPYMGEHPEYEGLFIATGHYRNGILLSPITGKL 360

GO        ISDLIMNK--EVNQDWLHAFRIDRKEAVQI 369
Node 5    MADLIEGKPPEADLKLLEPFSLDRFQATTV 390
```

Fig. 3. CONSURF analysis of GO. (A) Phylogenetic tree of glycine oxidases; the nodes represent different ancestors. (B) Amino acid alignment between the GO wild-type and the most probable ancestral sequence of node 5 (see text for details). Multiple alignment was performed using CLUSTALW (http://npsa-pbil.ibcp.fr/cgi-bin/npsa_automat.pl?page=npsa_clustalw.html) at the Pole Bioinformatique Lyonnais. The target amino acid positions for site-saturation mutagenesis are colored by their conservation scores as in Fig. 1: purple, conserved residues; blue, conservation scores > 70%; orange, conservation scores > 35%.

energies similar to those obtained using the wild-type GO (-3.9 kcal·mol^{-1} for both ligands, Table 4).

M49 side chain is at ~ 4.3 Å and ~ 4.7 Å from the αC of glycine or from the $-CH_3$ of sarcosine, respectively. In this case, too, a direct involvement of this residue in the binding of the substrate is unlikely. Accordingly, the M49L GO variant docking analysis with both ligands also showed energy levels close to those of the wild-type GO (-3.8 and -4.1 kcal·mol^{-1}, respectively; Table 4).

The discrepancy between the docking analysis (which does not show any alteration in the mode and energy of glycine or sarcosine binding in the active site of H244K and M49L variants with respect to wild-type

Table 4. Docking simulations between GO (wild-type, H244K or M49L variants) and glycine or sarcosine (see text for details). During the production of the 3D model of the H244K GO variant, potential alternative conformations of the loop 51–56 generated by the SWISS-PDBVIEWER software were taken into consideration; these alternative models are identified as conf.1 and conf.2. Binding energies (and corresponding K_d values) of ligands to the active site of variant proteins with alternative conformations (in comparison with the one observed with the wild-type GO) are represented in parentheses. Values cited in the text are reported in bold. n.a., not applicable; n.d., not determined.

Target structure				Ligand: glycine			Ligand: sarcosine		
PDB code	GO variant	Loop 51–56 conformation	Active site waters	Runs (correct/total)	Binding energy (kcal·mol^{-1})	K_d (mM)	Runs (correct/total)	Binding energy (kcal·mol^{-1})	K_d (mM)
1NG3	WT	WT	No	0/1	n.a.	n.a.	0/1	n.a.	n.a.
1NG3	WT	WT	Yes	0/1	n.a.	n.a.	4/7	−3.9	1.4
1RYI	WT	WT	No	4/4	−3.6	2.3	0/1	n.a.	n.a.
1RYI	WT	WT	Yes[a]	1/1	−3.7	1.9	1/1	**−4.1**	**0.9**
1RYI	WT	WT	Yes	1/1	**−3.9**	**1.4**	1/1	−2.5	14.8
1NG3	H244K	WT	Yes	2/2	−3.5 (−3.8)	2.7 (1.6)	2/2	−3.6 (−4.3)	2.3 (0.7)
1NG3	H244K	conf.1	Yes	2/2	−3.5 (−3.8)	2.7 (1.6)	2/2	−3.9 (−4.2)	1.4 (0.8)
1NG3	H244K	conf.1	Yes	1/4	−3.7 (−3.7)	1.9 (1.9)	4/4	−4.3 (−4.1)	0.7 (0.9)
1RYI	H244K	conf.1	Yes	3/3	**−3.9**	1.4	3/3	−2.6	12.5
1RYI	H244K	conf.1	Yes[a]	3/4	−3.8	1.6	3/3	**−3.9**	1.4
1NG3	H244K	conf.2	Yes[b]	3/3	−1.5	79.6	n.d.	n.d.	n.d.
1NG3	H244K	conf.2	Yes	0/3	n.a.	n.a.	0/3	−2.3	20.6
1RYI	H244K	conf.2	Yes	0/3	n.a.	n.a.	n.d.	n.d.	n.d.
1RYI	H244K	conf.2	Yes	3/3	−3.9	1.38	2/3	−3.4	3.2
1RYI	H244K	conf.2[c]	Yes	0/3	n.a.	n.a.	n.d.	n.d.	n.d.
1RYI	H244K	conf.2[c]	Yes	3/3	−4.0	1.2	3/3	−3.4	3.2
1NG3	M49L	WT	Yes	3/3	−3.4	3.2	3/4	−3.8	1.6
1RYI	M49L	WT	Yes	4/4	**−3.8**	1.6	3/3	−3.6	2.3
1RYI	M49L	WT	Yes[a]	1/3	−3.5	2.7	3/3	**−4.1**	0.9

[a] A water molecule close to the αNH$_2$ group of glycine was removed (Fig. 1, yellow water).

[b] An additional water molecule was modeled at the active site of this GO variant using the position of the water molecule reported in PDB 1RYI as a reference (depicted in yellow in Fig. 1).

[c] Orientation of R329 side chain of this GO variant was re-modeled using the orientation of the same side chain observed in PDB 1NG3 as a reference.

GO) and the experimental kinetic properties (Table 2) might depend on the fact that docking analysis estimates binding energy in a system at equilibrium, while K_m depends on the rate constant of several steps of the catalyzed reaction. Specifically, for the reaction catalyzed by GO the $K_{m,Gly}$ steady-state parameter corresponds to $k_4(k_{-1} + k_2)/(k_1 \cdot k_{-2})$, where k_1 and k_{-1} are the rate constants for substrate binding and dissociation to the oxidized enzyme form, k_2 and k_{-2} are the rate constants of the flavin reduction step, and k_4 is the rate constant for imino acid dissociation from the reoxidized GO [15]; in particular for wild-type GO $k_2 \gg k_{cat}$ and $k_{cat} \sim k_4$. We thus propose that the experimentally observed changes in $K_{m,app}$ for the two tested substrates in GO variants probably arise from alterations in several single kinetic constants and do not represent a change in the affinity for these substrates at equilibrium, i.e. in the true K_d ($= k_{-1}/k_1$) value. This result resembles that reported for a D-amino acid oxidase variant with 10-fold lower K_m for O_2, which resulted from combining the modifications of specific kinetic steps, each with a small amplitude [16].

Glycine and sarcosine detection

Based on the kinetic properties reported in Table 2 and the kinetic efficiency shown in the dot plot reported in Fig. 2B, the H244K GO variant was selected to develop a biosensor to specifically assay glycine: $K_{m,app}$ for glycine was the lowest among the identified GO variants, and the kinetic efficiency was 6.6-fold higher than for sarcosine. Similarly, the M49L variant was selected for the biosensor aimed to assay sarcosine: the very low $K_{m,app}$ for such a substrate was coupled to a 16.3-fold higher kinetic efficiency than on glycine.

Noteworthy is that all the evolved GO variants show only marginal, if any, activity with D-alanine. The kinetic efficiency ($k_{cat,app}/K_{m,app}$) parameter of the few GO variants active on D-alanine was 0.07, 0.02–0.05 and 0.01 mM^{-1}·s^{-1} for the H244K-R, M49I-L and H244K/M261R variants, respectively (versus 0.01 for the wild-type GO) [4,5]. In particular, the kinetic efficiency of the two selected GO variants for D-alanine is 100- and 500-fold lower than for the compounds to be assayed. Moreover, the wild-type and all the

evolved GO variants show no activity on L-alanine and creatinine (up to 10 mM final substrate concentration).

On the basis of these results, the M49L and H244K selected GO variants were employed in a device made of two commercially available, disposable cuvettes for fluorescence analysis filled with the Nile Red fluorescence transducer and the sensing GO enzyme, respectively (Fig. 4). The fluorimeter records the fluorescence intensity emission of the dye transducer, which is modulated by the different intensity of light absorbed by the GO enzyme in the free (oxidized) and substrate-bound (reduced) state. In fact, the change in spectral features of the enzyme reacted with different concentrations of substrate affects the amount of excitation light reaching the dye transducer, thus tuning its fluorescence emission [17]. To set up the system, the fluorescence intensity emission of the dye transducer (Nile Red) was monitored during the absorbance change in GO from the oxidized to reduced form: by adding an excess of glycine/sarcosine anaerobically to the system to reduce the FAD cofactor of GO, an increase in dye fluorescence is detected in 1 s, reaching a value stable over time (Fig. 4B). This finding is the result of a decrease in the absorbance intensity at 450 nm of GO in the reduced form [4,5], which leads to an increase in photon absorbance by the dye.

The analytical systems were then calibrated for measuring the emission fluorescence at 623 nm after adding standard glycine/sarcosine solutions (1–20 μM range) under anaerobic conditions. The emission values were plotted as a function of substrate concentrations and fitted by means of a Michaelis–Menten equation (Fig. 4C). In the presence of glycine as substrate, wild-type GO shows a $K_{m,app}$ of 11 ± 0.7 μM and the H244K variant a $K_{m,app}$ of 1 ± 0.3 μM; the observed 10-fold lower $K_{m,app}$ value is in good agreement with the kinetic parameters determined for H244K and wild-type GO (Table 2). The detection limit is ≤ 0.5 μM. Similarly, a $K_{m,app}$ ~ 2 μM is observed for M49L GO and sarcosine (Fig. 4C), again in agreement with the kinetic data determined with the oxygen consumption assay (Table 2).

We tested the utility of the GO-based detection system in applications requiring assessment of glycine or sarcosine level in cells stably expressing D-amino acid oxidase (DAAO), i.e. the enzyme that degrades the neuromodulator D-serine *in vivo* [18]. The standard assay for glycine requires the derivatization of the amino acid followed by separation (and quantification) by means of HPLC on a C8 column, each run requiring 60 min. In real time the H244K GO-based system determined a glycine concentration of 7.5 ± 0.6 μM (n = 6), compared with a figure of 6.7 ± 1.4 μM by

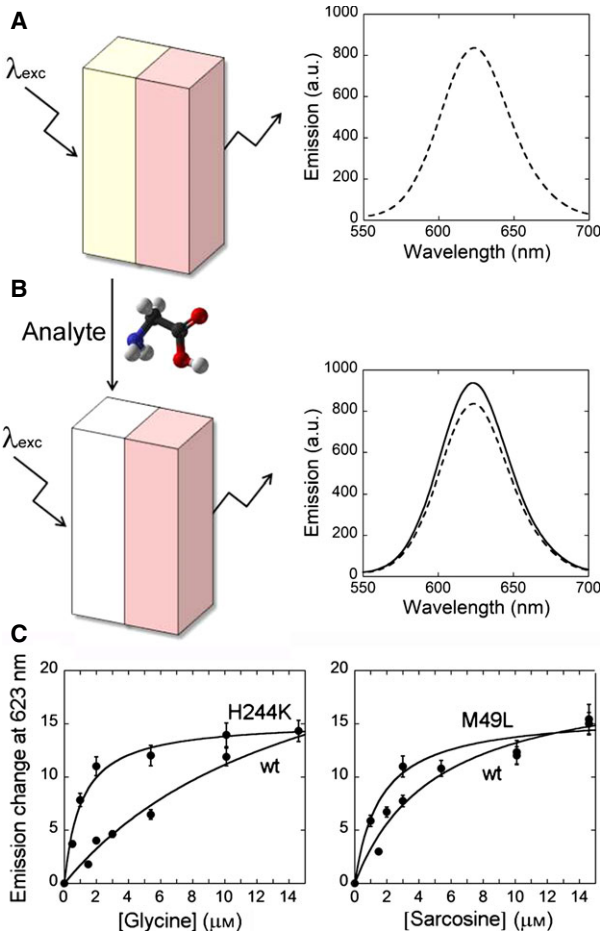

Fig. 4. Schematic representation of the biosensor for fluorimetric determination of glycine and sarcosine. Yellow, working cuvette (containing 0.1 μM GO variants and the substrate glycine/sarcosine); pink, dye-labeled cuvette (3 nM Nile Red). (A), (B) The fluorescence intensity of the dye transducer (Nile Red) is recorded during the change from the oxidized (dotted line, A) to the reduced form of GO (continuous line, B), after the anaerobic addition of the substrate. (C) Calibration plots for the detection of glycine and sarcosine based on change in fluorescence intensity in the presence of increasing glycine (left) or sarcosine (right) concentrations (n = 3).

HPLC analysis. The exogenous addition of 1.0 μM was fully quantified by the biosensor. The M49L GO-based system did not assay sarcosine in the biological sample (levels were below the detection limit) and estimated a concentration of 0.95 ± 0.11 μM after adding 1.0 μM exogenous sarcosine; this result demonstrates that this analytical system is suitable to assay the physiologically occurring concentration of sarcosine in prostate cancer patients, estimated at ~ 1.7 μM [19]. For the system based on H244K GO the response due to the presence of sarcosine was ≤ 20% of the value measured with the same concentration of glycine; a similar response was apparent for the M49L GO biosensor on

glycine versus sarcosine. Interestingly, the assay based on H244K GO variant allowed the glycine concentration in human plasma to be quantified: a value of 130 ± 18 μM was determined ($n = 6$), in good agreement with those reported in the literature [20].

Discussion

Modulation of glycine concentration is considered a main goal of modern neurochemistry since the relative contribution of glycine and D-serine to NMDAR activity in different brain regions is of central relevance for understanding neurotransmission mechanisms under both physiological and pathological conditions [2,21]. Accordingly, a specific biosensor for detecting glycine in biological fluids is of utmost importance. On the other hand, sarcosine is an isomer of alanine; previous studies proposing sarcosine as a cancer biomarker were challenged because the level of alanine in urine is higher than that of sarcosine and the analytical methods employed could not distinguish between these isomers [22].

The structural and functional information available on GO prompted us to consider this flavoenzyme as a starting point for evolving variants with improved properties of biotechnological interest. Unfortunately, GO is a poor biocatalyst: k_{cat} is significantly lower than the median turnover number of known enzymes (0.6 versus 10 s^{-1}) and the kinetic efficiency is also lower (860 versus 10^5 $M^{-1} \cdot s^{-1}$) – for both parameters GO is below the average and the range for ~ 60% of known enzymes [23].

In an attempt to evolve GO from *Bacillus subtilis* to obtain an enzyme with a higher catalytic efficiency on glycine and sarcosine, a semi-rational design approach based on site-saturation mutagenesis was employed. Based on *in silico* analysis, site-saturation mutagenesis was performed at 11 positions of the active site (Fig. 1). Screening results confirm that R302 contributes significantly to substrate binding and N330 is instead involved in cofactor binding (the N330P substitution resulted in the isolation of a variant GO in the apoprotein form). Substitution of M261 marginally altered the kinetic properties of GO, whereas replacement of A54 with an acidic or basic residue significantly decreased the substrate affinity (Table 2). In contrast, introduction of a basic residue at position 244 (which contains an asparagine in the most probable ancestral sequence according to the phylogenetic analysis, Fig. 3B) improved the kinetic efficiency constant on glycine compared with wild-type GO (up to 11-fold for the H244K variant, Fig. 2A) by decreasing the $K_{m,app}$ value (up to 5-fold for the H244K GO variant, Table 2). Previous site-directed mutagenesis studies showed that the H244F substitution increased product release and negatively affected the rate of flavin reduction with sarcosine, without affecting the turnover number [24]. Moreover, the presence of an alanine residue at site 244 had a synergistic effect on the activity of GO on glyphosate as substrate by increasing the stability of variants containing multiple replacements [11]. Worthy of note is that the 244 residue is the tip of the β-hairpin directly facing the α2-α3 loop, which seems to change its conformation according to the presence and the nature of the ligand in the binding site [11]. The same investigation showed a positive effect on glyphosate binding to GO by introducing an arginine at the active site entrance (i.e. at positions 51 and 54, part of the α2-α3 loop). The present study highlights a main effect of substitutions at positions 51 and 54 on the affinity and maximal activity for the small-size substrates investigated.

Results from phylogenetic analysis and site-saturation mutagenesis studies suggested that A54R, H244K and M261R substitutions be combined: (a) the H244K/M261R GO variant shows a 5-fold increase in the kinetic efficiency constant on both glycine and sarcosine, thus resulting in an enzyme useful for oxidizing and/or assaying both substrates; (b) the A54R/H244K GO variant shows the highest maximal activity on both glycine and sarcosine but is associated with a decreased substrate affinity and protein stability (Tables 2 and 3).

In order to develop novel enzyme-based biosensors, the H244K and M49L GO variants were selected to assay glycine and sarcosine, respectively, based on their kinetic properties and substrate specificity (Fig. 2B). Importantly, our enzymatic system is not affected by either the L-isomer (estimated in the 60–270 μM range in urine) or the D-isomer of alanine.

In order to rapidly assay the content of glycine/sarcosine in biological samples, a simple disposable pilot biosensor characterized by low cost and ease of use was set up based on the two selected GO variants. This new system was based on tuning the fluorescence emission of a commercial dye according to the different intensity of light absorbed by a small amount (0.1 μM) of GO in the presence of the analyte. The fluorescence intensity emission of Nile Red dye transducer is proportional to the amount of excitation light, which in turn depends on the concentration of analyte and its binding to GO [17]. The novel sensing assay shows a detection limit ≤ 0.5 μM (slightly lower than commercial assay kits) and was used to assay glycine and sarcosine in biological fluid, i.e. in a U87 glioblastoma cell line used to study the modulation of D-serine level by the catabolic enzyme D-amino acid oxidase

[18,25]; D-serine and glycine are alternative ligands required, together with glutamate, to activate NMDARs [21,26]. The glycine concentration detected by the H244K GO-based assay was in good agreement with the value obtained by using the reference HPLC method (7.5 versus 6.7 μM, respectively) but in 1 s, compared with the 60 min required by chromatographic separation. The M49L GO-based assay highlighted the very low amount of sarcosine in the cell line used and fully quantified sarcosine when exogenously added to the biological sample.

In conclusion, the high sensitivity of fluorescence detection combined with the use of evolved GO variants makes this device a powerful basis for developing a new generation of biosensors as alternatives to the time-consuming and expensive conventional methods.

Experimental procedures

Molecular modeling studies

Automated ligand docking was performed by using AUTODOCK VINA, a package based on an iterated local search global algorithm [27,28]. PYMOL software was used to analyze docking results and to identify noncovalent interactions between the protein moiety and glycine or sarcosine (www.pymol.org/). The structure of wild-type GO (PDB 1RYI) was used for all docking simulations, and was also taken as the starting point for preparing the models of GO variants (H244K and M49L) by using the MUTAGENESIS WIZARD tool of PYMOL. For each substitution, the rotamer with the highest occurrence in proteins and which did not clash with adjacent residues was selected. The choice of the correct rotamer was also confirmed by performing the same 'virtual' mutation using SWISS-PDBVIEWER software [29].

Site-directed and site-saturation mutagenesis

Single-point mutations were generated by site-directed mutagenesis using the QuikChange Site-Directed Mutagenesis Kit (Agilent Technologies, Santa Clara, CA, USA) and the pT7-His-GO plasmid [4]. Site-saturation mutagenesis experiments were carried out at different positions using the same procedure as for site-directed mutagenesis, a set of degenerated synthetic oligonucleotides (Table 5) and the pT7-His-GO plasmid encoding for wild-type or selected GO variants as template (see Table 1). The PCR products (full-length plasmids) were used to transform JM109 *E. coli* cells (the cloning host strain); the plasmid DNA was then pooled and transferred to BL21(DE3)pLysS *E. coli* cells (the expression host strain); recombinant cells were used for the screening procedure as detailed below. For each position, ~ 280 clones were screened (Table 5), a number that gives a probability of 96% that every single amino acid is introduced at the desired position [30], and 10 clones were sequenced to verify the mutagenesis efficiency. The introduction of the mutations was confirmed by automated DNA sequencing.

Screening for evolved GO variants

The mutant libraries obtained from the site-saturation mutagenesis approach were screened by means of a rapid colorimetric assay based on the determination of hydrogen peroxide produced by single recombinant *E. coli* cultures (1 mL) grown overnight to saturation at 37 °C in a 2 mL deep-well plate (Eppendorf, Hamburg, Germany) in LB medium to which 0.5 mM isopropyl-β-D-thiogalactopyranoside was added and then incubated at 30 °C for 5 h. An aliquot (100 μL) of each culture was transferred to a single well of a microtiter plate; 100 μL of lysis buffer (50 mM disodium pyrophosphate buffer, pH 8.5, 1 mM EDTA, 100 mM NaCl, 20% CelLytic B and 1 $mg{\cdot}mL^{-1}$ deoxyribonuclease I) was added, and the cells were incubated at 37 °C for 30 min. The GO activity was assayed on crude extracts (200 μL) by adding 1.8 mM glycine (or 1.8 mM sarcosine), 0.2% Triton X-100, 0.3 $mg{\cdot}mL^{-1}$ *o*DNS and 1 $unit{\cdot}mL^{-1}$ horseradish peroxidase in 100 mM disodium pyrophosphate buffer, pH 8.5 (the 'peroxidase-*o*DNS assay'). The time course of the absorbance change at 450 nm was followed at room temperature by a microtiter plate reader (Sunrise, Tecan, Männedorf, Switzerland) and compared with that of control cells (expressing wild-type GO or lacking the GO-encoding pT7 plasmid). This screening analysis was performed by using the automated system epMotion 5075 (Eppendorf). The clones that outperformed the control were selected for sequencing and biochemical characterization.

Enzyme expression and purification

The pT7 expression plasmids coding for His-tagged GO wild-type and different GO variants were transferred to the host BL21(DE3)pLysS *E. coli* strain. Recombinant cells were grown at 37 °C in Terrific Broth medium containing 100 $\mu g{\cdot}mL^{-1}$ ampicillin and 34 $\mu g{\cdot}mL^{-1}$ chloramphenicol, and protein expression was induced in the exponential phase of growth by adding isopropyl-β-D-thiogalactopyranoside to a final concentration of 0.5 mM [5]. The cells were then grown at 30 °C and collected after 18 h by centrifugation. Crude extracts were prepared by sonication (four cycles of 30 s each) of the cell paste suspended with 50 mM disodium pyrophosphate buffer, pH 8.5, containing 5 mM EDTA, 2 μM FAD, 5 mM 2-mercaptoethanol, 0.7 $\mu g{\cdot}mL^{-1}$ pepstatin, 1 mM phenylmethanesulfonyl fluoride and 10 $\mu g{\cdot}mL^{-1}$ deoxyribonuclease I (2–3 mL of buffer per gram of *E. coli* cells). The insoluble fraction of the lysate was removed by centrifugation at 39 000 ***g*** for 1 h [5]. The recombinant GO proteins were purified from the crude extracts by using HiTrap chelating chromatography

Table 5. Vectors and oligonucleotides used as 5′ and 3′ primers in the site-saturation mutagenesis performed at different amino acid positions.

Vector	AA position	Primers	Screened clones (number)
pT7-His-GO	49	M49_up 5′-CGACAAGTGCCGCTGCCGGANNNCTGGGCGCCC-3′	282
		M49_dw 5′-GGGCGCCCAGNNNTCCGGCAGCGGCACTTGTCG-3′	
	51	G51_up 5′-GCCGCTGCCGGAATGCTGNNNGCCCATGCCGAATGC-3′	
		G51_dw 5′-GCATTCGGCATGGGCNNNCAGCATTCCGGCAGCGGC-3′	
	54	A54_up 5′-GGAATGCTGGGCGCCCATNNNGAATGCGAGGAACG-3′	
		A54_dw 5′-CGTTCCTCGCATTCNNNATGGGCGCCCAGCATTCC-3′	
	95	M95_up 5′-GGCAGCATAACGGCGGTNNNTTTAAGCTTGCATTTTC-3′	
		M95_dw 5′-GAAAATGCAAGCTTAAANNNACCGCCGTTATGCTGCC-3′	
	241	Y241_up 5′-CGCTGACAAAAACGCTTNNNCATGATCACTGC-3′	
		Y241_dw 5′-GCAGTGATCATGNNNAAGCGTTTTTGTCAGCG-3′	
	244	H244_up 5′-CGCTTTACCATGATNNNTGCTATATCGTACCG-3′	
		H244_dw 5′-CGGTACGATATAGCANNNATCATGGTAAAGCG-3′	
	246	Y246_up 5′-CCATGATCACTGCNNNATCGTACCGAG-3′	
		Y246_dw 5′-CTCGGTACGATNNNGCAGTGATCATGG-3′	
	261	M261_up 5′-GTCGGCGCGACANNNAAGCCGGGGGACTGG-3′	
		M261_dw 5′-CCAGTCCCCCGGCTTNNNTGTCGCGCCGA-3′	
	302	R302_up 5′-GGGCGGGACTCNNNCCGGGAACAAAGG-3′	
		R302_dw 5′-CCTTTGTTCCCGGNNNGAGTCCCGCCC-3′	
	329	R329_up 5′-CGGCTGGCCATTTCNNNAACGGGATCCTGC-3′	
		R329_dw 5′-GCAGGATCCCGTTNNNGAAATGGCCAGCCG-3′	
	330	N330_up 5′-GGCCATTTCAGANNNGGGATCCTGCTTGCTCC-3′	
		N330_dw 5′-GGAGCAAGCAGGATCCCNNNTCTGAAATGGCC-3′	
pT7-His-GO-H244K	49	M49_up 5′-CGACAAGTGCCGCTGCCGGANNNCTGGGCGCCC-3′	279
		M49_dw 5′-GGGCGCCCAGNNNTCCGGCAGCGGCACTTGTCG-3′	
	54	A54_up 5′-GGAATGCTGGGCGCCCATNNNGAATGCGAGGAACG-3′	
		A54_dw 5′-CGTTCCTCGCATTCNNNATGGGCGCCCAGCATTCC-3′	
	246	HK_Y246_up 5′-CGCTTTACCATGATAAATGCNNNATCGTACCG-3′	
		HK_Y246_dw 5′-CGGTACGATNNNGCATTTATCATGGTAAAGCG-3′	
pT7-His-GO-A54R/H244K	49	M49_up 5′-CGACAAGTGCCGCTGCCGGANNNCTGGGCGCCC-3′	279
		M49_dw 5′-GGGCGCCCAGNNNTCCGGCAGCGGCACTTGTCG-3′	

(GE Healthcare, Little Chalfont, UK) as reported previously [5,31]. The purified GO variants were then equilibrated with 50 mM disodium pyrophosphate buffer, pH 8.5, and 10% glycerol [24].

Assay for GO activity (and substrate specificity)

Standard GO activity was assayed with an oxygen electrode on 10 mM glycine as substrate at pH 8.5, 25 °C and at air saturation ($[O_2]$ = 0.253 mM) [5]. One unit of GO corresponds to the amount of enzyme that uses 1 μmol of oxygen (or produces 1 μmol of hydrogen peroxide) in 1 min at 25 °C. Apparent kinetic parameters were determined by the same polarographic assay, employing different concentrations of the substrates glycine or sarcosine (0–100 mM) at a fixed oxygen concentration (air saturation).

Enzyme characterization

Spectral experiments were carried out at 15 °C in 50 mM disodium pyrophosphate buffer, pH 8.5, 10% glycerol. Extinction coefficients of the GO variants were determined by heat denaturation of the enzymes (at 95 °C for 10 min) and using the absorption coefficient for free FAD of 11.3 mM^{-1} cm^{-1} [4].

The stability of selected GO variants was determined by temperature ramp experiments measuring protein fluorescence changes with an FP-750 spectrofluorimeter (Jasco, Cremello, Italy) equipped with a thermostatted cell holder and using a 3-mL cuvette. Fixed wavelength measurements were taken at 340 nm (excitation wavelength 298 nm). The experiments were performed using a software-driven, Peltier-based temperature controller which allowed a temperature gradient of 0.5 °C·min^{-1} [12]. The denaturation curve was used to extrapolate the melting temperature (T_m value) of the enzymes, as described elsewhere [12].

Ancestral reconstruction

For phylogenetic analysis, the amino acid sequence of wild-type GO was used as input for the web-based tool CONSURF (http://consurf.tau.ac.il/) [32]. The multiple sequence alignment of homologous sequences was used to generate a phy-

logenetic tree using FASTML [33]; all ancestral sequences for the various nodes were predicted and the most probable ancestral sequence was predicted.

Biosensor preparation

A simple fluorescence-based biosensor was built by employing two commercially glued fluorescence cuvettes. The 'dye-labeled cuvette' was filled with a solution of the dye Nile Red (1 $\mu g \cdot mL^{-1}$ in ethanol) and the 'working cuvette' with 50 mM disodium pyrophosphate buffer, pH 8.5. The fluorescence emission spectra were recorded from 500 to 700 nm, with excitation at 450 nm, by using a Jasco FP-750 spectrofluorimeter. Quenching of the initial fluorescence intensity was observed when the enzyme was added to the working cuvette; the intensity decrease depended both on the enzyme concentration and the amount of the fluorophore [17]. For these measurements, GO (oxidized form) at a final concentration of 0.1 μM was added to the working cuvette. Then, increasing amounts of glycine or sarcosine were added to the working cuvette in the absence of oxygen (by fluxing the cuvettes with purified N_2) at room temperature. The fluorescence emission values were recorded at 623 nm.

Glycine/sarcosine detection in biological samples

All experiments were performed using a U87 human glioblastoma cell line stably expressing human DAAO [25]. Cellular amino acids were extracted as described previously [18]: 2.5×10^5 U87 cells were resuspended in 1 mL of ice-cold 5% trichloroacetic acid, sonicated and centrifuged for 45 min at 16 000 ***g***. For the HPLC assay, the soluble fraction was extracted with water-saturated ether, neutralized and derivatized with *o*-phthaldialdehyde/*N*-acetyl-L-cysteine. Glycine was resolved by HPLC chromatography on a 5-μm Waters C8 reversed-phase column (Waters Corp., Milford, MA, USA) eluted under isocratic conditions (100 mM sodium acetate buffer, pH 6.2, 1% tetrahydrofuran at 1 $mL \cdot min^{-1}$; 60 min per run). For biosensor measurements, the soluble fraction was extracted with water-saturated ether, resuspended in 50 mM disodium pyrophosphate buffer, pH 8.5, and added to the working cuvette containing the GO enzyme variants. Amino acids were extracted from human plasma samples as described before [34]: plasma (20 μL) was mixed vigorously with methanol (180 μL) and centrifuged for 5 min at 15 000 ***g***. For measurements of glycine content, the supernatant was added to the working cuvette containing the H244K GO variant. Glycine/sarcosine amounts were determined according to calibration curves obtained with standard glycine and sarcosine.

Acknowledgements

This work was supported by a grant from the Fondo di Ateneo per la Ricerca (Università degli studi dell' Insubria). We are grateful for the support from Consorzio Interuniversitario per le Biotecnologie CIB and to Gianluca Tomasello for help in docking analyses.

Author contributions

ER and LF performed protein engineering experiments and biochemical characterization; MV and LuP performed protein expression and purification trials; GM carried out docking experiments; ER, AV, SD developed the pilot biosensor; LoP conceived the project; ER and LoP wrote the paper. All authors have read and approved the final manuscript.

References

1 Dannhardt G & Kohl BK (1998) The glycine site on the NMDA receptor: structure–activity relationships and possible therapeutic applications. *Curr Med Chem* **5**, 253–263.
2 Beyoglu D & Idle JR (2012) The glycine deportation system and its pharmacological consequences. *Pharmacol Ther* **135**, 151–167.
3 Sreekumar A, Poisson LM, Rajendiran TM, Khan AP, Cao Q, Yu JD, Laxman B, Mehra R, Lonigro RJ, Li Y *et al.* (2009) Metabolomic profiles delineate potential role for sarcosine in prostate cancer progression. *Nature* **457**, 910–914.
4 Job V, Marcone GL, Pilone MS & Pollegioni L (2002) Glycine oxidase from *Bacillus subtilis*. Characterization of a new flavoprotein. *J Biol Chem* **277**, 6985–6993.
5 Job V, Molla G, Pilone MS & Pollegioni L (2002) Overexpression of a recombinant wild-type and His-tagged *Bacillus subtilis* glycine oxidase in *Escherichia coli*. *Eur J Biochem* **269**, 1456–1463.
6 Pollegioni L, Molla G, Sacchi S, Rosini E, Verga R & Pilone MS (2008) Properties and applications of microbial D-amino acid oxidases: current state and perspectives. *Appl Microbiol Biotechnol* **78**, 1–16.
7 Pollegioni L, Motta P & Molla G (2013) L-amino acid oxidase as biocatalyst: a dream too far? *Appl Microbiol Biotechnol* **97**, 9323–9341.
8 Mortl M, Diederichs K, Welte W, Molla G, Motteran L, Andriolo G, Pilone MS & Pollegioni L (2004) Structure–function correlation in glycine oxidase from *Bacillus subtilis*. *J Biol Chem* **279**, 29718–29727.
9 Settembre EC, Dorrestein PC, Park JH, Augustine AM, Begley TP & Ealick SE (2003) Structural and mechanistic studies on ThiO, a glycine oxidase essential for thiamin biosynthesis in *Bacillus subtilis*. *Biochemistry* **42**, 2971–2981.
10 Pollegioni L & Molla G (2011) New biotech applications from evolved D-amino acid oxidases. *Trends Biotechnol* **29**, 276–283.

11 Pedotti M, Rosini E, Molla G, Moschetti T, Savino C, Vallone B & Pollegioni L (2009) Glyphosate resistance by engineering the flavoenzyme glycine oxidase. *J Biol Chem* **284**, 36415–36423.
12 Caldinelli L, Iametti S, Barbiroli A, Bonomi F, Fessas D, Molla G, Pilone MS & Pollegioni L (2005) Dissecting the structural determinants of the stability of cholesterol oxidase containing covalently bound flavin. *J Biol Chem* **280**, 22572–22581.
13 Caldinelli L, Pedotti M, Motteran L, Molla G & Pollegioni L (2009) FAD binding in glycine oxidase from *Bacillus subtilis*. *Biochimie* **91**, 1499–1508.
14 Alcolombri U, Elias M & Tawfik DS (2011) Directed evolution of sulfotransferases and paraoxonases by ancestral libraries. *J Mol Biol* **411**, 837–853.
15 Molla G, Motteran L, Job V, Pilone MS & Pollegioni L (2003) Kinetic mechanisms of glycine oxidase from *Bacillus subtilis*. *Eur J Biochem* **270**, 1474–1482.
16 Rosini E, Pollegioni L, Ghisla S, Orru R & Molla G (2009) Optimization of D-amino acid oxidase for low substrate concentrations – towards a cancer enzyme therapy. *FEBS J* **276**, 4921–4932.
17 Strianese M, Varriale A, Staiano M, Pellecchia C & D'Auria S (2011) Absorption into fluorescence. A method to sense biologically relevant gas molecules. *Nanoscale* **3**, 298–302.
18 Cappelletti P, Campomenosi P, Pollegioni L & Sacchi S (2014) The degradation (by distinct pathways) of human D-amino acid oxidase and its interacting partner pLG72 – two key proteins in D -serine catabolism in the brain. *FEBS J* **281**, 708–723.
19 Cernei N, Zitka O, Ryvolova M, Adam V, Masarik M, Hubalek J & Kizek R (2012) Spectrometric and electrochemical analysis of sarcosine as a potential prostate carcinoma marker. *Int J Electrochem Sci* **7**, 4286–4301.
20 Neeman G, Blanaru M, Bloch B, Kremer I, Ermilov M, Javitt DC & Heerco-Levy U (2005) Relation of plasma glycine, serine, and homocysteine levels to schizophrenia symptoms and medication type. *Am J Psychiatry* **162**, 1738–1740.
21 Pollegioni L & Sacchi S (2010) Metabolism of the neuromodulator D-serine. *Cell Mol Life Sci* **67**, 2387–2404.
22 Issaq HJ & Veenstra TD (2011) Is sarcosine a biomarker for prostate cancer? *J Sep Sci* **34**, 3619–3621.
23 Bar-Even A, Noor E, Savir Y, Liebermeister W, Davidi D, Tawfik DS & Milo R (2011) The moderately efficient enzyme: evolutionary and physicochemical trends shaping enzyme parameters. *Biochemistry* **50**, 4402–4410.
24 Boselli A, Rosini E, Marcone GL, Sacchi S, Motteran L, Pilone MS, Pollegioni L & Molla G (2007) Glycine oxidase from *Bacillus subtilis*: role of histidine 244 and methionine 261. *Biochimie* **89**, 1372–1380.
25 Sacchi S, Cappelletti P, Giovannardi S & Pollegioni L (2011) Evidence for the interaction of D-amino acid oxidase with pLG72 in a glial cell line. *Mol Cell Neurosci* **48**, 20–28.
26 Martineau M, Baux G & Mothet JP (2006) D-serine signalling in the brain: friend and foe. *Trends Neurosci* **29**, 481–491.
27 Golden E, Paterson R, Tie WJ, Anandan A, Flematti G, Molla G, Rosini E, Pollegioni L & Vrielink A (2013) Structure of a class III engineered cephalosporin acylase: comparisons with class I acylase and implications for differences in substrate specificity and catalytic activity. *Biochem J* **451**, 217–226.
28 Trott O & Olson AJ (2010) Software news and update AutoDock Vina: improving the speed and accuracy of docking with a new scoring function, efficient optimization, and multithreading. *J Comput Chem* **31**, 455–461.
29 Guex N & Peitsch MC (1997) SWISS-MODEL and the Swiss-PdbViewer: an environment for comparative protein modeling. *Electrophoresis* **18**, 2714–2723.
30 Pollegioni L, Lorenzi S, Rosini E, Marcone GL, Molla G, Verga R, Cabri W & Pilone MS (2005) Evolution of an acylase active on cephalosporin C. *Protein Sci* **14**, 3064–3076.
31 Fantinato S, Pollegioni L & Pilone MS (2001) Engineering, expression and purification of a His-tagged chimeric D-amino acid oxidase from *Rhodotorula gracilis*. *Enzyme Microb Tech* **29**, 407–412.
32 Landau M, Mayrose I, Rosenberg Y, Glaser F, Martz E, Pupko T & Ben-Tal N (2005) ConSurf 2005: the projection of evolutionary conservation scores of residues on protein structures. *Nucleic Acids Res* **33**, W299–W302.
33 Pupko T, Pe'er I, Shamir R & Graur D (2000) A fast algorithm for joint reconstruction of ancestral amino acid sequences. *Mol Biol Evol* **17**, 890–896.
34 Huang Y, Nishikawa T, Satoh K, Iwara T, Fukushima T, Santa T, Homma H & Imai K (1998) Urinary excretion of D-serine in human: comparison of different ages and species. *Biol Pharm Bull* **21**, 156–162.